

Catalytic Activation of H₂ under Mild Conditions by an [FeFe]-Hydrogenase Model via an Active μ -Hydride Species

Ning Wang,^{†,‡} Mei Wang,^{*,†} Ying Wang,[§] Dehua Zheng,[†] Hongxian Han,^{||} Mårten S. G. Ahlquist,[§] and Licheng Sun^{*,†,⊥}

[†]State Key Laboratory of Fine Chemicals, DUT-KTH Joint Education and Research Center on Molecular Devices, Dalian University of Technology (DUT), Dalian 116024, China

[‡]School of Chemistry and Chemical Engineering, Henan University of Technology, Zhengzhou 450001, China

[§]School of Biotechnology, KTH Royal Institute of Technology, Stockholm SE-106 91, Sweden

^{||}State Key Laboratory of Catalysis, Dalian Institute of Chemical Physics, Dalian 116023, China

[⊥]Department of Chemistry, KTH Royal Institute of Technology, Stockholm SE-100 44, Sweden

Supporting Information

ABSTRACT: A [FeFe]-hydrogenase model (**1**) containing a chelating diphosphine ligand with a pendant amine was readily oxidized by Fc⁺ (Fc = Cp₂Fe) to a Fe^{II}Fe^I complex ([**1**)⁺, which was isolated at room temperature. The structure of [**1**)⁺ with a semibridging CO and a vacant apical site was determined by X-ray crystallography. Complex [**1**)⁺ catalytically activates H₂ at 1 atm at 25 °C in the presence of excess Fc⁺ and P(*o*-tol)₃. More interestingly, the catalytic activity of [**1**)⁺ for H₂ oxidation remains unchanged in the presence of ca. 2% CO. A computational study of the reaction mechanism showed that the most favorable activation free energy involves a rotation of the bridging CO to an apical position followed by activation of H₂ with the help of the internal amine to give a bridging hydride intermediate.

[FeFe]-hydrogenases ([FeFe]-H₂ases) are enzymes that catalyze both proton reduction and H₂ oxidation. These reactions are closely related to energy storage by production of H₂ from water splitting and energy release by H–H bond cleavage in a fuel cell. With a strong desire to replace the commonly used Pt by earth-abundant metal-based catalysts, structural and functional mimicking of the [FeFe]-H₂ase active site has attracted extensive attention since the crystal structure of [FeFe]-H₂ases was unveiled.¹ The key structural factors of the [FeFe]-H₂ase active site are a diiron dithiolate core, an amine cofactor in the S-to-S bridge, and a 4Fe4S cluster tethered to the diiron core through a cysteine residue (Figure 1). Direct biophysical evidence, experimental results, and theoretical calculations revealed that

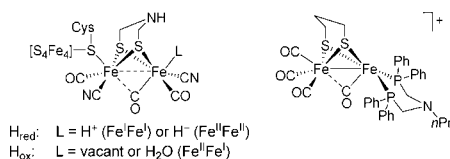


Figure 1. H_{red} and H_{ox} states of the [FeFe]-H₂ase active site (left) and the model complex [**1**)⁺ (right).

the amine cofactor acts as a shuttle for protons being transferred to and from the distal Fe and the 4Fe4S cluster functions as an electron transfer relay to complete the redox processes at the diiron core. The proton-coupled electron transfer process provides a low-energy pathway for H–H bond cleavage and formation at the diiron dithiolate core. This enables [FeFe]-H₂ases to serve as highly active catalysts for both proton reduction and H₂ oxidation.²

Over the past decade, studies of [FeFe]-H₂ase mimics have been mostly concentrated on the H_{red} state (Figure 1) for proton reduction³ and H₂ activation under photolysis,⁴ while modeling of the H_{ox} state for H₂ oxidation has been paid less attention. The first experimental evidence for the formation of the Fe^{II}Fe^I bridging-CO complex was observed in situ from the one-electron oxidation of a diiron carbonyl cyanide precursor bearing a thioether group.⁵ Later, two structurally characterized mixed-valence diiron models of H_{ox} were reported by the groups of Darensbourg and Rauchfuss.⁶ The H_{ox} mimics reported to date are diiron dithiolate complexes either bearing the special σ ligands 1,3-bis(2,4,6-trimethylphenyl)imidazol-2-ylidene (IMes) and *cis*-1,2-C₂H₂(PPh₂)₂ (dppv) or featuring a bulky bridge, 2,2-dimethyl-1,3-propanedithiolate (dmpdt).^{7,8} There are only three examples of the activation of H₂ using Fe^{II}Fe^I complexes, reported by Rauchfuss and co-workers. The models for H_{ox} containing an azadithiolate (adt) bridge react very slowly with H₂ under high pressure to give μ -H complexes,⁹ while in the presence of a supplemental oxidant the activation of H₂ occurs under mild conditions at significantly higher rates.¹⁰ Recently, a functional model of H_{ox} containing both an internal amine and a redox-active unit, Cp^{*}Fe(C₅Me₄CH₂PET₂) (FcP^{*}) (Cp^{*} = C₅Me₅),¹¹ was reported to be active for the oxidation of 1 atm H₂ at 25 °C in the presence of excess FcBAR^F₄ [Fc = Cp₂Fe, Ar^F = 3,5-(CF₃)₂C₆H₃] and P(*o*-tol)₃, giving 0.4 turnover/h in 5 h.

We previously reported a diiron complex bearing a pendant amine in a chelating diphosphine ligand, [(μ -pdt){Fe(CO)₃}-{Fe(CO)(PNP)}] (**1**) [pdt = propane-1,3-dithiolate, PNP = Ph₂PCH₂N(*n*Pr)CH₂PPh₂], and its doubly protonated species [1(H_NH_μ)]²⁺ (Scheme 1).¹² An interesting feature of this

Received: August 13, 2013

Published: September 3, 2013

complex is the distinct reactivity of the μ -H atoms in $[\mathbf{1}(\text{H}_\mu)]^+$ and $[\mathbf{1}(\text{H}_\text{N}\text{H}_\mu)]^{2+}$ from those in diiron complexes bearing an adt bridge.¹³ In the continuous work, we studied the one-electron oxidation of $\mathbf{1}$ and the activation of H_2 by $[\mathbf{1}]^+$ (Figure 1). To our delight, we found that $[\mathbf{1}]^+$ can indeed activate H_2 in a catalytic manner under mild conditions in the presence of excess oxidant and base.

First of all, the cyclic voltammogram of $\mathbf{1}$ in CH_2Cl_2 shows a fully reversible one-electron event at $E_{1/2} = -0.22$ V vs $\text{Fc}^{+/0}$ and an irreversible event at $E_{\text{pa}} = 0.80$ V vs $\text{Fc}^{+/0}$ [Figure S1 in the Supporting Information (SI)] assigned to the $[\mathbf{1}]^{+/0}$ and $[\mathbf{1}]^{2+/+}$ couples, respectively. On the basis of electrochemical results, Fc^+ was chosen as the oxidant, as it can oxidize $\mathbf{1}$ to $[\mathbf{1}]^+$ but cannot further oxidize $[\mathbf{1}]^+$ to $[\mathbf{1}]^{2+}$. Chemical oxidation of $\mathbf{1}$ by 1 equiv of FcX ($X = \text{PF}_6, \text{BAR}_4^{\text{F}}$) under argon immediately led to the disappearance of the ν_{CO} bands of $\mathbf{1}$ ($\nu_{\text{CO}} = 2025, 1953, \text{ and } 1898 \text{ cm}^{-1}$)¹² accompanied by the appearance of three new bands at higher energy ($\nu_{\text{CO}} = 2081, 2022, \text{ and } 1900 \text{ cm}^{-1}$). The apparent blue shifts of the first two ν_{CO} bands (Figure 2a) suggest the

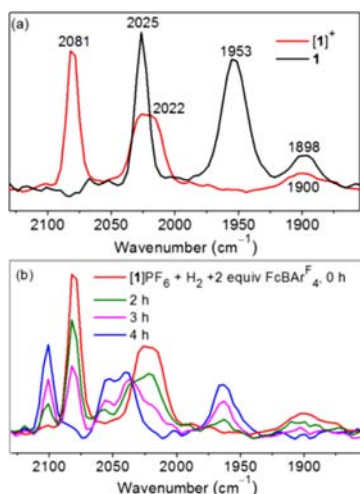


Figure 2. (a) Selected regions of the IR spectra of $\mathbf{1}$ and $[\mathbf{1}]^+$. (b) In situ IR changes of the reaction of $[\mathbf{1}]\text{PF}_6$ with 1 atm H_2 in CH_2Cl_2 containing 2 equiv of $\text{FcBAR}_4^{\text{F}}$ at 25 °C.

formation of a mixed-valence species ($[\mathbf{1}]^+$). The weak band at 1900 cm^{-1} is indicative of a semibridged CO ligand, as reported previously in $\text{Fe}^{\text{II}}\text{Fe}^{\text{I}}$ models (Table S1 in the SI).^{6,7,10} The IR spectral changes demonstrated that $\mathbf{1}$ was completely converted to $[\mathbf{1}]^+$ within 5 min in the presence of 1 equiv of FcPF_6 or $\text{FcBAR}_4^{\text{F}}$ in CH_2Cl_2 (Figure S2). When 1 equiv of the reductant Cp_2Co was added to the solution of $[\mathbf{1}]^+$, $\mathbf{1}$ was quantitatively recovered.

The X-band EPR spectrum of a CH_2Cl_2 /toluene solution of $[\mathbf{1}]\text{BAR}_4^{\text{F}}$ at -163 °C (Figure S3) displayed three peaks with principal g values simulated to 2.139, 2.019, and 2.018. The g values of $[\mathbf{1}]^+$ are similar to those observed for H_{ox} from $[\text{FeFe}]\text{-H}_2\text{ases}$ ($g_1 = 2.10, g_2 = 2.04, g_3 = 1.99$).¹⁴ The EPR and IR spectra together support the assignment of $[\mathbf{1}]^+$ as $[(\mu\text{-pdt})\{\text{Fe}^{\text{II}}(\text{CO})_3\}\text{-}\{\text{Fe}^{\text{I}}(\text{CO})(\text{PNP})\}]^+$.

The IR spectrum of $[\mathbf{1}]\text{PF}_6$ in CH_2Cl_2 remained unchanged for several hours and $[\mathbf{1}]\text{BAR}_4^{\text{F}}$ with a bulky counterion was stable in CH_2Cl_2 for several days at room temperature under a N_2 atmosphere. Crystals of $[\mathbf{1}]\text{BAR}_4^{\text{F}}$ were obtained from CH_2Cl_2 /hexane at room temperature. X-ray diffraction analysis (Figure 3 and Tables S2 and S3) showed that $[\mathbf{1}]^+$ has a similar framework as other reported H_{ox} models,^{6,7} consisting of an oxidized

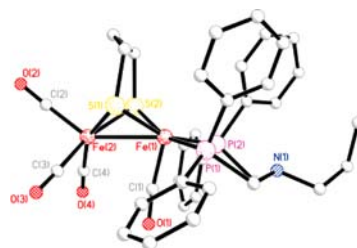


Figure 3. X-ray crystal structure of the cation in $[\mathbf{1}]\text{BAR}_4^{\text{F}}$. Selected distances (Å) and angles (deg): $\text{Fe}(1)\text{-Fe}(2), 2.5730(8)$; $\text{Fe}(1)\cdots\text{N}(1), 3.7990(8)$; $\text{Fe}(1)\text{-C}(1), 1.779(4)$; $\text{Fe}(2)\text{-C}(1), 2.755(6)$; $\text{Fe}(2)\text{-Fe}(1)\text{-C}(1), 76.13(13)$; $\text{Fe}(1)\text{-C}(1)\text{-O}(1), 172.8(4)$; $\text{Fe}(2)\text{-C}(1)\text{-O}(1), 122.1(2)$.

$\text{Fe}(\text{CO})_3$ moiety and a rotated $\text{Fe}(\text{CO})(\text{PNP})$ unit with an open apical site on the Fe center. The Fe–Fe distance of $2.5730(8)$ Å in $[\mathbf{1}]^+$ is slightly longer than that in the neutral complex $\mathbf{1}$ [Fe–Fe $2.5565(7)$ Å]. The semibridging character of the CO is evident from the relatively long $\text{Fe}(2)\text{-C}(1)$ distance of $2.755(6)$ Å compared with the $\text{Fe}(1)\text{-C}(1)$ distance of $1.779(4)$ Å and the obvious difference in the $\text{Fe}(1)\text{-C}(1)\text{-O}(1)$ [$172.8(4)^\circ$] and $\text{Fe}(2)\text{-C}(1)\text{-O}(1)$ [$122.1(2)^\circ$] angles. Although in the solid state the nitrogen of the $\text{FeP}_2\text{C}_2\text{N}$ ring of $[\mathbf{1}]^+$ has its lone pair pointing away from the Fe–Fe bond, the variable-temperature ^{31}P and ^1H NMR spectra of $\mathbf{1}$ indicate a fluxional process associated with the $\text{FeP}_2\text{C}_2\text{N}$ ring in solution at room temperature (Figure S4). In fact, in our previous work we demonstrated the coexistence of the H_N -endo/exo isomers of $[\mathbf{1}(\text{H}_\text{N}\text{H}_\mu)]^{2+}$ in solution generated by protonation of $\mathbf{1}$.¹² Such a fluxional process of a $\text{FeP}_2\text{C}_2\text{N}$ ring was also found for DuBois' mononuclear iron complexes.¹⁵

Considering the good thermostability of $[\mathbf{1}]^+$ and the special reactivity of the μ -H species derived from $\mathbf{1}$, we anticipated that $[\mathbf{1}]^+$ could promote H_2 activation. Monitoring of the reaction by IR spectroscopy showed that the in situ-generated $[\mathbf{1}]\text{BAR}_4^{\text{F}}$ reacted smoothly with 1 atm H_2 at 25 °C in the presence of 2 equiv of FcPF_6 , and the reaction finished over a period of 4 h (Figure S5). The influence of the counterion (PF_6^- or $\text{BAR}_4^{\text{F}-}$) on the reaction of $[\mathbf{1}]^+$ with H_2 in the presence of Fc^+ was studied by in situ IR spectroscopy as well. The results indicated that both the counterion of $[\mathbf{1}]^+$ and the counterion of the oxidant have an apparent influence on the $[\mathbf{1}]^+$ -catalyzed H_2 oxidation reaction. With more PF_6^- in the solution, the reaction rate was considerably higher, but the stability of $[\mathbf{1}]^+$ was apparently decreased. It might be possible that PF_6^- helps to shuttle protons to facilitate the heterolytic cleavage of H_2 .¹⁶ The cations formed in solution were deprotonated instantly upon addition of excess base [$\text{P}(o\text{-tol})_3$], and the neutral complex $\mathbf{1}$ was recovered in 50–100% yield (Figure S5) depending on the counterion in solution. In case of PF_6^- , about 50% of $[\mathbf{1}]^+$ decomposed after reaction for 2 h, while no decomposition was observed after reaction for 7.5 h with $\text{BAR}_4^{\text{F}-}$ as the sole counterion (Figures S6 and S7).

After the reaction with H_2 , the ν_{CO} bands of $[\mathbf{1}]^+$ completely disappeared and a set of new ν_{CO} bands at 2103, 2055, 2043, and 1968 cm^{-1} emerged in the IR spectrum (Figure 2b). In addition, three typical signals at δ 37.3, 46.2, and 58.5 in the ^{31}P NMR spectrum of the resulting solution (Figure S8) are attributed to the products $[\mathbf{1}(\text{H}_\mu)]^+$, $[\mathbf{1}(\text{H}_\text{N}\text{H}_\mu)]^{2+}$, and $[\mathbf{1}(\text{H}_\text{N})]^+$, respectively, according to the ^{31}P NMR data for the same cations formed by treatment of $\mathbf{1}$ with 1 or 2 equiv of Brønsted acid.^{12,13,17} Accordingly, the ^1H NMR spectrum of the solution resulting from the reaction of $\mathbf{1}$ with 1 atm H_2 in CD_2Cl_2

containing 2 equiv of FcPF_6 (Figure S9) showed three signals at δ -13.20 , -13.75 , and -14.07 for the μ -H atoms derived from H_2 uptake by $[\mathbf{1}]^+$, attributed to $[\mathbf{1}(\text{H}_\mu)]^+$ and the $\text{H}_{\text{N-exo}}$ and $\text{H}_{\text{N-endo}}$ isomers of $[\mathbf{1}(\text{H}_\text{N}\text{H}_\mu)]^{2+}$, respectively. The formation of $[\mathbf{1}(\text{H}_\text{N}\text{H}_\mu)]^{2+}$ in the reaction of $[\mathbf{1}]^+$ with H_2 provides clear support for heterolysis of the H–H bond at the diiron center. The molecular structure of $[\mathbf{1}(\text{H}_\text{N}\text{H}_\mu)]^{2+}$ formed by double protonation was determined by spectroscopic studies and single-crystal X-ray analysis in our previous work,¹² which showed that the distance between H_μ^- and H_N^+ is 3.934 Å.

A comparative study of the analogous complex $[(\mu\text{-pdt})\{\text{Fe}(\text{CO})_3\}\{\text{Fe}(\text{CO})(\text{dppp})\}]$ (**2**) [$\text{dppp} = \text{Ph}_2\text{P}(\text{CH}_2)_3\text{PPh}_2$], which lacks the internal base, was performed under the same conditions used for the oxidation of H_2 by **1**. The in situ IR spectra showed that **2** was rapidly oxidized to $[\mathbf{2}]^+$ by Fc^+ but that $[\mathbf{2}]^+$ did not react with 1 atm H_2 at 25 °C in CH_2Cl_2 in the presence of Fc^+ (Figure S10). This result indicates the significant role of the amine built into the chelating diphosphine ligand in the oxidation of H_2 at diiron models. Although the internal amine of **1** is positioned differently from that of the adt bridge in the conventional models of $[\text{FeFe}]\text{-H}_2$ ases, it acts as a proton shuttle functionally like the adt cofactor.

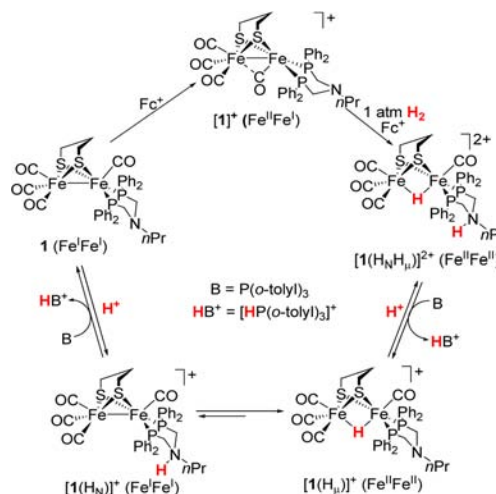
A convenient method for analyzing the heterolytic activation of H_2 is to trap protons as $[\text{HP}(\text{o-tol})_3]^+$.¹⁰ Excitingly, when the oxidation of H_2 by $[\mathbf{1}]\text{PF}_6$ was carried out in the presence of 20 equiv of FcBARF_4 and 20 equiv of $\text{P}(\text{o-tol})_3$ under 1 atm H_2 at 25 °C for 10 h, the catalytic conversion of $\text{P}(\text{o-tol})_3$ to $[\text{HP}(\text{o-tol})_3]^+$ was detected by ^{31}P NMR spectroscopy (Figure S11), giving a turnover of 6.2 ± 0.1 moles of H_2 consumed per mole of **1**. This is the first example to show that a simple H_{ox} model becomes catalytically active for the oxidation of H_2 under mild conditions in the presence of an oxidant through activation of the μ -H with a specially designed built-in amine in the secondary coordination sphere of a diiron complex. The reported turnover number for H_2 uptake for the H_{ox} model $[(\mu\text{-adtBn})\{\text{Fe}(\text{CO})_2(\text{FcP}^*)\}\{\text{Fe}(\text{CO})(\text{dppv})\}]$ is 2 in 5 h under similar conditions.¹¹ Other previously reported H_{ox} models bearing an adt bridge can activate H_2 only stoichiometrically under similar conditions because of the inertness of the μ -H species formed in H_2 activation.^{10,11} The amine unit in the adt bridge, which is at the opposite position of the μ -H, cannot activate the μ -H of a diiron dithiolate complex. The unique activity of the μ -H atoms in $[\mathbf{1}(\text{H}_\mu)]^+$ and $[\mathbf{1}(\text{H}_\text{N}\text{H}_\mu)]^{2+}$ was verified in our previous work in terms of the facile deprotonation of the μ -H in the presence of weak bases or even a trace amount of water and the rapid H/D exchange of the μ -H with deuterons in solution.^{13,14}

When CO gas was bubbled into the CH_2Cl_2 solution of $[\mathbf{1}]^+$ at -70 °C, changes in the ν_{CO} region were immediately observed in the in situ IR spectra, with the ν_{CO} absorptions of $[\mathbf{1}]^+$ finally shifting to 2052 and 1990 cm^{-1} over ca. 2 h (Figure S12), indicating the easy coordination of CO at the open apical site of the rotated Fe^{I} unit of $[\mathbf{1}]^+$.⁸ The reversibility of this process was evidenced by the quick and complete recovery of the characteristic ν_{CO} absorptions of $[\mathbf{1}]^+$ when the solution of the in situ-formed $[\mathbf{1}(\text{CO})]^+$ was removed from the cooling bath and allowed to stand at room temperature. Consequently, no inhibiting effect on the catalytic activity of $[\mathbf{1}]^+$ for H_2 oxidation was observed in the presence of ca. 2% CO (see the SI), a major impurity in H_2 fuels derived from reformed hydrocarbons or biomass.

According to the experimental results obtained from the present and previous work as well as theoretical calculations,^{18–20} a possible pathway for catalytic activation of H_2 by

1 in the presence of an oxidant and a base is proposed in Scheme 1. Complex **1** is readily oxidized to $[\mathbf{1}]^+$ by a one-electron

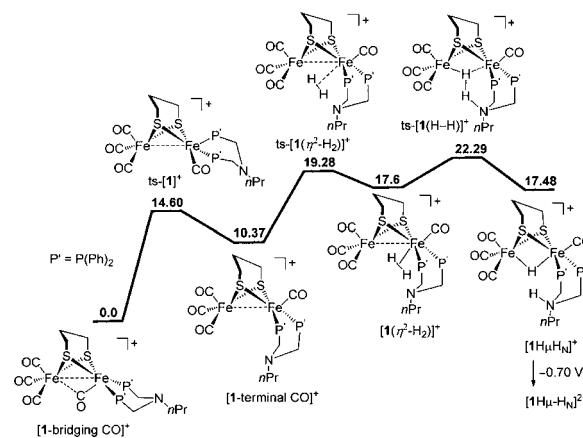
Scheme 1. Proposed Pathway for H_2 Oxidation by **1 in the Presence of Fc^+ and $\text{P}(\text{o-tol})_3$**



process, while $[\mathbf{1}]^+$ cannot be further oxidized to $[\mathbf{1}]^{2+}$ in the presence of extra Fc^+ .⁹ In another aspect, $[\mathbf{1}]^+$ is inactive for the activation of H_2 under mild conditions in the absence of a supplemental oxidant. $[\mathbf{1}]^+$ can react with H_2 in the presence of excess Fc^+ to form the μ -H complex $[\mathbf{1}(\text{H}_\text{N}\text{H}_\mu)]^{2+}$, which is readily converted to $[\mathbf{1}(\text{H}_\mu)]^+$ and $[\mathbf{1}(\text{H}_\text{N})]^+$ via partial deprotonation by $\text{P}(\text{o-tol})_3$ and then back to **1** by further deprotonation to fulfill a complete catalytic cycle. Fast deprotonation of $[\mathbf{1}(\text{H}_\mu)]^+$ is attributed to the internal amine of the PNP ligand. The μ -H is first deprotonated by the internal base, and this is followed by proton transfer from the internal to the external base.¹⁸ This detour deprotonation pathway of $[\mathbf{1}(\text{H}_\mu)]^+$ is also supported by the fact that the analogous μ -H complex $[\mathbf{2}(\text{H}_\mu)]^+$ cannot be deprotonated in the presence of excess $\text{P}(\text{o-tol})_3$ or Et_3N .

To further understand the details of H_2 activation by $[\mathbf{1}]^+$, we performed a computational study of the mechanism for the reaction of $[\mathbf{1}]^+$ and H_2 to afford $[\mathbf{1}(\text{H}_\mu\text{H}_\text{N})]^{2+}$ (Scheme 2, Figure

Scheme 2. Profile of Calculated Relative G Values for H_2 Activation by $[\mathbf{1}]^+$ in CH_2Cl_2 ^a



^aThe relative Gibbs free energies are given in kcal mol^{-1} , and the oxidation potential is in V vs $\text{Fc}^{+/0}$.

S13, and Table S4). The favorable reaction path starts from rotation of the semibringing CO to an apical position with a free energy barrier of 14.60 kcal mol⁻¹ via ts-[1]⁺. The intermediate [1-terminal CO]⁺ is then capable of binding H₂ from the down site to form [1(η²-H₂)]⁺ via ts-[1(η²-H₂)]⁺, overcoming a barrier of 8.91 kcal mol⁻¹. With the involvement of the internal amine N, the calculated activation free energy associated with heterolytic cleavage of the H–H bond in [1(η²-H₂)]⁺ via ts-[1-H–H]⁺ is only 4.69 kcal mol⁻¹. The thereby-generated [1H_μH_N]⁺ is converted to [1H_μH_N]²⁺ by one-electron oxidation, for which a potential of –0.70 V vs Fc^{+/0} was calculated. The total free energy barrier for this H₂ activation pathway is 22.29 kcal mol⁻¹. The results show that the inclusion of the internal amine in [1]⁺ is important for efficient H₂ activation. We also note that the activation of H₂ directly at [1-bridging CO]⁺ to form a terminal hydride (*t*-H) intermediate is less favored and has a total activation free energy of 26.8 kcal mol⁻¹. Although the diferrous ammonium *t*-H complex is assumed to be an initially formed intermediate in both the oxidation of H₂ and the reduction of protons at diiron azadithiolate models,^{9–11,21} the *t*-H species was observed neither in the activation of H₂ by [1]⁺ nor in the protonation processes of **1** and an analogous diiron complex [(μ-pdt){Fe(CO)₃}{Fe(CO)(PNP')}] (**3**) [PNP' = Ph₂PCH₂N(Me)CH₂PPh₂].¹⁷ It has been reported that for the process of proton reduction to H₂ at **3**, the energy barrier for *t*-H formation by proton transfer from the ammonium of the PNP' ligand is ca. 3 times higher than the corresponding barrier for μ-H formation.¹⁹ The down-site attack of D₂ or H₂ at an iron center of the [FeFe]-H₂ase model was also proposed for the catalytic process of H/D exchange by μ-H diiron dithiolate complexes.²²

In conclusion, complex **1** bearing a chelating diphosphine ligand with a pendant amine can be rapidly oxidized by Fc⁺ to give [1]⁺, which has been structurally characterized. Of particular note, [1]⁺, as a model of H_{ox}, exhibits catalytic activity for H₂ oxidation in the presence of excess oxidant and base, and the catalytic activity of [1]⁺ for H₂ oxidation is sustained in the presence of ca. 2% CO. The activity of the μ-H atoms in [1(H_μ)]⁺ and [1(H_NH_μ)]²⁺ is distinct from those in diiron dithiolate models containing an adt bridge because of the short distance between the built-in amine of the diphosphine ligand and the μ-H. Comparative studies of the analogous complexes **1** and **2** clearly indicated that the internal base in the secondary coordination sphere is indispensable for the activation of H₂ under mild conditions. These results show that on the basis of the essential factors in the structure of [FeFe]-H₂ase active site, simple and improved functional models can be designed as catalysts for both reduction of protons to H₂ and oxidation of H₂ to protons.

■ ASSOCIATED CONTENT

● Supporting Information

Procedures and additional data. This material is available free of charge via the Internet at <http://pubs.acs.org>.

■ AUTHOR INFORMATION

Corresponding Authors

symbueno@dlut.edu.cn
lichengs@kth.se

Notes

The authors declare no competing financial interest.

■ ACKNOWLEDGMENTS

We are grateful to the National Natural Science Foundation of China (21101057, 21373040, 21120102036), the Basic Research Program of China (2014CB239402), the Knut and Alice Wallenberg Foundation for financial support of this work. Y.W. and M.S.G.A. thank Vetenskapsrådet and EU-Erasmus Mundus.

■ REFERENCES

- (1) (a) Peters, J. W.; Lanzilotta, W. N.; Lemon, B. J.; Seefeldt, L. C. *Science* **1998**, *282*, 1853. (b) Nicolet, Y.; Piras, C.; Legrand, P.; Hatchikian, C. E.; Fontecilla-Camps, J. C. *Structure* **1999**, *7*, 13.
- (2) (a) Nicolet, Y.; Lacey, A. L.; Vernede, X.; Fernandez, V. M.; Hatchikian, E. C.; Fontecilla-Camps, J. C. *J. Am. Chem. Soc.* **2001**, *123*, 1596. (b) Pandey, A. S.; Harris, T. V.; Giles, L. J.; Peters, J. W.; Szilagyi, R. K. *J. Am. Chem. Soc.* **2008**, *130*, 4533. (c) Fan, H.-J.; Hall, M. B. *J. Am. Chem. Soc.* **2001**, *123*, 3828.
- (3) (a) Capon, J.-F.; Gloaguen, F.; Pétilion, F. Y.; Schollhammer, P.; Talarmin, J. *Coord. Chem. Rev.* **2009**, *253*, 1476. (b) Felton, G. A. N.; Mebi, C. A.; Petro, B. J.; Vannucci, A. K.; Evans, D. H.; Glass, R. S.; Lichtenberger, D. L. *J. Organomet. Chem.* **2009**, *694*, 2681. (c) Tschierlei, S.; Ott, S.; Lomoth, R. *Energy Environ. Sci.* **2011**, *4*, 2340.
- (4) (a) Heiden, Z. M.; Zampella, G.; De Gioia, L.; Rauchfuss, T. B. *Angew. Chem., Int. Ed.* **2008**, *47*, 9756. (b) Matthews, S. L.; Heinekey, D. M. *Inorg. Chem.* **2011**, *50*, 7925.
- (5) Razavet, M.; Borg, S. J.; George, S. J.; Best, S. P.; Fairhurst, S. A.; Pickett, C. J. *Chem. Commun.* **2002**, 700.
- (6) (a) Liu, T.; Darensbourg, M. Y. *J. Am. Chem. Soc.* **2007**, *129*, 7008. (b) Justice, A. K.; Rauchfuss, T. B.; Wilson, S. R. *Angew. Chem., Int. Ed.* **2007**, *46*, 6152.
- (7) (a) Justice, A. K.; Gioia, L. D.; Nilges, M. J.; Rauchfuss, T. B.; Wilson, S. R.; Zampella, G. *J. Am. Chem. Soc.* **2008**, *130*, 7405. (b) Singleton, M. L.; Bhuvanesh, N.; Reibenspies, J. H.; Darensbourg, M. Y. *Angew. Chem., Int. Ed.* **2008**, *47*, 9492.
- (8) (a) Justice, A. K.; Nilges, M. J.; Rauchfuss, T. B.; Wilson, S. R.; De Gioia, L.; Zampella, G. *J. Am. Chem. Soc.* **2008**, *130*, 5293. (b) Thomas, C. M.; Liu, T.; Hall, M. B.; Darensbourg, M. Y. *Inorg. Chem.* **2008**, *47*, 7009.
- (9) Olsen, M. T.; Barton, B. E.; Rauchfuss, T. B. *Inorg. Chem.* **2009**, *48*, 7507.
- (10) Camara, J. M.; Rauchfuss, T. B. *J. Am. Chem. Soc.* **2011**, *133*, 8098.
- (11) Camara, J. M.; Rauchfuss, T. B. *Nat. Chem.* **2012**, *4*, 26.
- (12) Wang, N.; Wang, M.; Zhang, T.; Li, P.; Liu, J.; Sun, L. *Chem. Commun.* **2008**, 5800.
- (13) Wang, N.; Wang, M.; Liu, L.; Jin, K.; Chen, L.; Sun, L. *Inorg. Chem.* **2009**, *48*, 11551.
- (14) Albracht, S. P. J.; Roseboom, W.; Hatchikian, E. C. *J. Biol. Inorg. Chem.* **2006**, *11*, 88.
- (15) Henry, R. M.; Shoemaker, R. K.; DuBois, D. L.; DuBois, M. R. *J. Am. Chem. Soc.* **2006**, *128*, 3002.
- (16) (a) Heiden, Z. M.; Rauchfuss, T. B. *J. Am. Chem. Soc.* **2009**, *131*, 3593. (b) Macchioni, A. *Chem. Rev.* **2005**, *105*, 2039.
- (17) Ezzaher, S.; Capon, J.-F.; Gloaguen, F.; Pétilion, F. Y.; Schollhammer, P.; Talarmin, J. *Inorg. Chem.* **2009**, *48*, 2.
- (18) Wang, Y.; Wang, M.; Sun, L.; Ahlquist, M. S. G. *Chem. Commun.* **2012**, *48*, 4450.
- (19) Lounissi, S.; Zampella, G.; Capon, J.-F.; Gioia, L. D.; Matoussi, F.; Mahfoudhi, S.; Pétilion, F. Y.; Schollhammer, P.; Talarmin, J. *Chem.—Eur. J.* **2012**, *18*, 11123.
- (20) Wang, Y.; Ahlquist, M. S. G. *Dalton Trans.* **2013**, *42*, 7816.
- (21) (a) Barton, B. E.; Rauchfuss, T. B. *Inorg. Chem.* **2008**, *47*, 2261. (b) Barton, B. E.; Olsen, M. T.; Rauchfuss, T. B. *J. Am. Chem. Soc.* **2008**, *130*, 16834. (c) Olsen, M. T.; Rauchfuss, T. B.; Wilson, S. R. *J. Am. Chem. Soc.* **2010**, *132*, 17733.
- (22) (a) Zhao, X.; Georgakaki, I. P.; Miller, M. L.; Mejia-Rodriguez, R.; Chiang, C.-Y.; Darensbourg, M. Y. *Inorg. Chem.* **2002**, *41*, 3917. (b) Georgakaki, I. P.; Miller, M. L.; Darensbourg, M. Y. *Inorg. Chem.* **2003**, *42*, 2489.